Hysteresis between groundwater and surface water levels indicates the states of hydrological turnover affecting solute transport and redox processes

Lars Bäthke[1] and Tobias Schuetz[1]

[1] Department of Hydrology, Faculty of Regional and Environmental Sciences, University of Trier, Trier, Germany
Correspondence to: Lars Bäthke (baethke@uni-trier.de) and Tobias Schuetz (tobias.schuetz@uni-trier.de)

Abstract

Small streams are highly sensitive to variations in discharge, a sensitivity predicted to increase in future climate scenarios, impacting ecological health of streams and water management practices. Prolonged low-flow conditions alter groundwater-surface water (GW-SW) exchange patterns, leading to extended losing phases and a reduced duration of gaining periods. This study examines the relationship between hydrological turnover (HT) and stream-stage-groundwater-level hysteresis patterns under various system states in a third-order tributary of the River Mosel in Trier, Germany, using high-resolution stream-stage and groundwater-level data (GW1, GW2) together with complementary chemical observations collected over two years.

Our results reveal distinct seasonal dynamics in GW-SW exchange. Counterclockwise hysteresis, prevalent during summer and drought conditions, coincides with conditions indicative of hyporheic zone expansion and bank storage, potentially affecting flow paths and redox dynamics. We established a strong correlation between HT and hysteresis characteristics, identifying the h-index as a valuable diagnostic tool for tracking seasonal changes in GW-SW connectivity, storage and hyporheic zone behavior based on hydraulic preconditions.

As climate change intensifies drought conditions, the hyporheic zone will play a vital role in solute cycling and GW-SW connectivity. The h-index, combined with chemical and hydrological monitoring, provides a robust framework for understanding and predicting these dynamics in small stream ecosystems.

1 Introduction

The interaction between GW and SW systems has an impact on the dynamics of streamflow, solute transport, and nutrient cycling, with significant implications for water resource management and ecological health. Within the broader hydrological system, delays in streamflow response are closely linked to stream-catchment connectivity governing the timing and magnitude of water, solute, carbon, and nutrient exchanges between surface and groundwater. In combination, these factors significantly impact stream water quality and a catchment's response to rainfall events (e.g., Brunner et al., 2009, 2011; Covino et al., 2011; Zuecco et al., 2019). Connectivity patterns frequently manifest hysteretic behavior, a non-linear, loop-like relationship between dependent and independent variables such as groundwater levels and river state (e.g., Pavlin et al., 2021; Camporese et al., 2014; Penna et al., 2011; Outram et al., 2014; McGuire & McDonnell, 2010; Gelmini et al., 2022; Zuecco et al., 2016, 2019). Hysteresis describes how a system's response depends on both current inputs and prior states and are defined by non-linear behavior in response to inputs (e.g. Phillips 2003; Camporese et al., 2014). This "hysteretic" behavior, commonly observed in interactions between groundwater and surface water levels, reveals the complex interplay among storage capacities, groundwater hydraulics and flow dynamics (Zuecco et al., 2019). For example, hysteresis can manifest as a delayed groundwater response to surface water discharge variations (Zuecco et al., 2016; Pavlin et al., 2021), highlighting the impact of the variability of hydraulic gradients between steam and aquifer within a catchment (Welch et al. 2015). Temporally asynchronous water level changes characterize subsurface flow paths and generating characteristic hysteresis loops between surface and groundwater (Penna et al., 2011). An improved understanding of hysteretic behavior thus might enhance our understanding of stream flow exchange with the riverbanks and the hyporheic zone, a nonlinear mechanism involved in stream flow generation and its chemical signature (McGuire & McDonnell, 2010).

Within the context of GW-SW interaction, hyporheic exchange fluxes are modulated by event characteristics and groundwater preconditions (Trauth & Fleckenstein, 2017). Defined as the boundary between ground and surface waters, the hyporheic zone expands and contracts depending on the relative difference between groundwater levels and stream discharge (e.g., Wroblicky et al., 1998; Arntzen et al., 2006). Thus, significantly affecting exchange volumes (Candenas & Wilson, 2007; Malzone et al., 2016). An increase in stream stage typically increases the hyporheic volume, whereas it shrinks during recession or low flow conditions (Soulsby et al., 2001). Hyporheic exchange in the riparian zone induced by fluctuations in the stream stage are referred to as bank storage. This extends the hyporheic volume further into the stream bank, distinct from in-stream hyporheic exchange (Cooper & Rorabaugh, 1963). Bank storage often induces transport and mixing of chemical species between groundwater and surface waters, leading to processing of these solutes and a delayed return of these potentially modified chemicals (Gu et al., 2012). Bank storage-induced GW-SW mixing thus has the potential to alter solute fluxes out of the hyporheic zone, influencing the chemical signature of groundwater discharge (McCallum et al., 2010).

The interaction between stream and groundwater levels propagates surface water fluctuations into groundwater systems, enhancing GW-SW exchange (Xin et al., 2018). Tools such as the hysteresis index developed by Zuecco et al. (2016) and similar methods by Lloyd et al. (2016b) systematically quantify and compare hysteresis during runoff events. These tools support the classification and characterization of hydrological responses in catchments (Gelmini et al., 2022). However, stream flow responsiveness depends on multiple factors, such as local groundwater levels, with stream water level fluctuations modifying hydraulic gradients that drive GW-SW interactions at the stream-groundwater interface (Boano et al., 2014; Cardenas, 2008).

Several studies advocate that the exchange between GW and SW along streams needs to be addressed as bidirectional, consisting of gross gains and losses, with the cumulative bidirectional flux understood as a hydrological turnover (HT). HT is a major control on solute transport, influences in-stream ecological functions. Thus, HT shapes stream chemical signatures, making it a critical framework for understanding the bidirectional GW-SW interactions explored in this study (Payn et al., 2009, 2012; Covino et al., 2011; Mallard et al., 2014; Jimenez-Fernandez et al., 2022; Jähkel et al., 2022; Bäthke & Schuetz, 2024).

The process of GW-SW interaction in headwater streams integrates the movement of water masses between the near-stream aquifer, the hyporheic zone, and the stream channel (Payn et al., 2009; Ward et al., 2013, 2019). The link between bidirectional GW-SW interaction processes and local small scale groundwater gradient change, expressed in the hysteresis between near-stream groundwater and stream water levels, has not yet been fully explored.

Addressing this gap, this study examines how seasonal variations of stream stage and groundwater levels, hydraulic gradients, and bank storage extension, in conjunction with hysteretic behavior, influence HT [$\%/m^{-1}$] in a headwater stream. By quantifying hysteresis loops and HT over two seasons, we determine the impact of groundwater-surface water exchange variability on solute transport and stream chemistry. Through 68 hysteresis loops and 28 HT measurements, including nine during the 2020 drought, we analyze how HT and hysteresis characteristics respond to seasonality and hydraulic gradients. Stream and near-stream groundwater sampling (DOC, NO_3^-, Mn, Fe) reveal changes in redox zonation with hysteretic behavior. Silica serves as a proxy for groundwater, providing insights into subsurface contributions to stream chemistry. Potassium, as a local proxy for stream water, highlights the influence of GW-SW interactions on mixing and solute transport through the stream bank.

The objective of this study is to explore how seasonal changes in hydraulic conditions influence groundwater–surface water interactions in a headwater stream. We hypothesize that (1) the direction and magnitude of hysteresis between groundwater and stream water levels are indicative of seasonal hydrological states, and (2) consequently, the direction and magnitude of the hysteresis is related to hydrological turnover. thus facilitating (3) redox fluctuations creating oxic-anoxic transition in the riparian zone, shaping redox hot spots.

2 Materials and Methods

2.1 Study Area

The Olewigerbach is a third-order tributary of the River Mosel, located south of the city of Trier in southwest Germany. The catchment drains a 25 km² watershed with a total stream length of 14 km (Krein & Schorer, 2000). The elevation difference between the headwaters and the outlet is approximately 300 m. The stream has a pluvial regime, receiving an average annual precipitation of 745 mm and exhibiting a mean discharge of 106 l/s recorded between 2010 and 2023 at the study site. The catchment's geology is dominated by Devonian schists, primarily argillaceous slates. The shallow soil layer (~1.3 m) contains impermeable clay pockets underlain by colluvial or bedrock argillaceous slates (Krein & Symader, 2000). The study area is situated in the headwaters of the catchment at an elevation of approximately 290 m above sea level, characterized by steep hillslopes.

Drought conditions were defined as periods when streamflow fell below 5% (5.3 l/s) of the mean discharge, following thresholds set by Yevjevich (1967) and Zelenhasic & Salvai (1987).

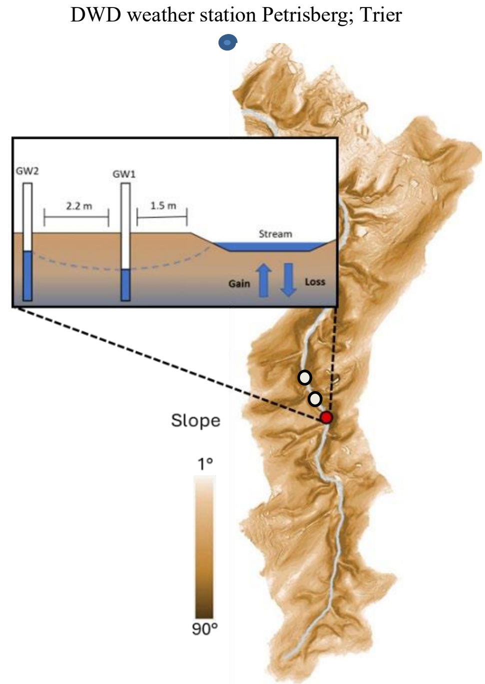

Figure 1: Spatial representation of topographic slopes of the Olewiger Bach catchment in the south of the city of Trier, Germany. Red: Gauging station with detailed sampling site sketch, with stream and sampling well setup. HT concept and groundwater connectivity through riparian zone. Blue: Location of the weather station. Grey: Location of additional sampling wells downstream.

2.2 Experimental Setup

Field measurements were conducted from 2020 to 2023. The dataset comprises 29 differential discharge gauging campaigns, utilizing NaCl slug injections, to HT during runoff events, over the stream section equipped with sampling wells. We monitored 68 runoff events with precipitation totals ranging up to 60 mm. Corresponding streamflow responses showed peak discharges between 20 and 700 L s^{-1}. Antecedent soil moisture conditions varied from dry at summer drought events to near saturation at winter events (Fig.3). While these event descriptions provide hydrological context, the classification of events in this study is based on hysteresis behaviour and HT rather than on precipitation or discharge metrics. Hysteresis loops were recorded based on stream water levels and groundwater levels measured at two groundwater wells (GW1 and GW2) located close to the stream (Figure 1). Groundwater levels were continuously logged in 10-minute intervals using Orpheus Mini Level Loggers (OTT GmbH).

At the upstream gauging station three piezometers were installed in a transect: one in the stream (289.47 m a.s.l.) and two at the groundwater wells, GW1 (288.63 m a.s.l.) and GW2 (288.65 m a.s.l.). GW1 is located 1.5 m from the streambank, and

GW2 is 3.7 m away. Groundwater levels were monitored at a depth of 1.3 m. From the hydrograph, 68 events were selected for hysteresis analysis using the h-index developed by Zuecco et al. (2016).

Table 1. Characteristics of events occurring prior to one or multiple tracer experiments. Duration of the Hydrograph response; Precipitation of the event; Mean discharge; Runoff volume and Runoff coefficient (Precipitation/Runoff volume)

Date	**Duration [h]**	**Precipitation [mm]**	**Mean Q [L/s]**	**Runoff vol. [m³]**	**Runoff coeff. [–]**
03-08-2020	70	3.8	13.5	3387	0.111
17-08-2020	24	8.3	14.5	1259	0.019
18-08-2020	48	2.2	0.1	10	0.001
02-09-2020	26	3.0	13	1240	0.596
24-09-2020	33	8.0	29.9	3529	0.056
06-10-2020	24	16.3	47.6	4110	0.031
09-10-2020	289	22.6	25.6	26684	0.148
23-10-2020	50	8.2	13.9	2524	0.039
08-02-2021	84	19.5	165.5	49981	0.321
13-03-2021	29	18.2	61.2	6336	0.044
19-03-2021	337	30.9	42.8	51882	0.210
11-04-2021	588	42.1	36.5	77294	0.229
26-05-2021	116	15.3	14.8	6171	0.050
04-06-2021	71	19.8	18.6	4777	0.030
29-06-2021	122	7.0	4.9	2159	0.039
05-07-2021	51	18.1	38.7	7114	0.049
27-07-2021	150	28.2	80.1	43289	0.192
08-08-2021	31	4.2	16.7	1861	0.056
26-11-2021	85	15.4	17.6	5376	0.044
07-12-2021	557	29.4	95.3	190892	0.813

Corresponding HT measurements were available for 29 of these events. We identified three severe drought periods i: March 27 to April 1, 2020; April 24 to September 28, 2020; and September 6 to October 20, 2021 (Figure 3). Precipitation and modelled soil moisture data (AMBAV, DWD) for the study area were obtained from the Deutscher Wetterdienst (DWD) weather station located near the Olewigerbach catchment (Station: Trier-Petrisberg; ID: 05100; https://opendata.dwd.de/climate_environment/). Streamflow data were monitored at the sampling site (Figure 1). We collected 144 water samples—48 each from the stream, GW1, and GW2—across three identical sampling spots, including two additional downstream locations without piezometers. The experimental infrastructure is drawn out in detail in Bäthke & Schuetz (2024).

Tracer Injection Protocol:

Instantaneous NaCl tracer injections were performed for HT estimation, during recession, utilizing salt dilution gauging (Day, 1976; Covino et al., 2011; Mallard et al., 2014). At the monitored stream section (~250 m) two independent discharge measurements were conducted, at the upstream and downstream ends of the stream reach. Injection distance for the measurement devices was approximately 30m (Bäthke & Schuetz, 2024). The Q_{loss} estimation is based on an additional tracer injection injected at the upstream site and measured at the downstream site, following the instructions of Payn et al. (2009). The wells are located in 1.5 m and 3 m lateral distance from the upstream measurement point.Electrical conductivity during tracer injections ranged from 203–320 µS/cm at baseline, with peaks 100–300 µS/cm above baseline levels.

- Injection mass ranged from 50 g to 2000 g of pre-dissolved NaCl, adjusted based on discharge and background conductivity.
- Breakthrough curves (BTCs) with peaks outside 1.25–2.0 times baseline conductivity was excluded or repeated.
- Measurements covered discharge rates from ~1 to 400 l/s.
- Conductivity was logged at 1-second intervals, except during extreme low-flow conditions (<5 l/s), when a 5-second resolution was used to conserve device storage capacity.

Electrical conductivity data were used to calculate mass equivalents, which were calibrated to determine HT (Eq. 1). The hyporheic zone covers the space between the riparian groundwater and the stream (Wondzell et al., 2011). Bäthke & Schuetz (2024) show that high HT magnitudes manifest in low variability between stream and groundwater silica concentrations, with silica concentrations serving as a proxy of prolonged contact with the subsurface (see as well e.g. Burns et al., 2003). Prior measurements have shown elevated potassium concentrations in the stream compared to groundwater, with its source upstream of the sampling site. Soils containing sufficient amounts of clay minerals (e.g. illite, vermiculite) may reduce the potassium in solution via sorption (Sparks & Huang, 1985). Thus, we measured potassium as a proxy for stream water. To study redox changes within the riparian zone, we conducted additional sampling for DOC, NO_3^-, Mn, Fe. Groundwater and stream samples were collected during stream flow recession towards baseflow conditions, immediately prior to the dilution gauging experiments (n = 48, table xx) and not during rainfall events. Laboratory analyses were carried out after filtration through a 0.45 µm glass fiber filter (Macherey & Nagel). Nitrate was determined by ion chromatography (±2%), potassium (±5%) and silica (±8%) by ion chromatography, iron and manganese (±5%) by atomic absorption spectroscopy (AAS, contrAA 300), and dissolved organic carbon (DOC) by combustion followed by IR detection (TOC analyzer, ±2%). Reported ± values represent the standard deviation of the replicate analyses.

2.2.1 Hydrologic Turnover

The conducted tracer experiments provided BTCs to quantify net changes in discharge along the reach (~250 m) as well as gross gains and losses of stream water to and from groundwater. With discharge estimation at the upper and lower end of the selected stream reach:

$$Q_i = \frac{M_i}{\int_0^t C_{M_i}(t)dt} \tag{1}$$

Where Q_i [l/s] is the discharge at location *i*, M_i [g] is initial tracer mass injected and $C_{M_i}(t)$ [g/l] the integrated tracer concentration from the BTC. Hydrological turnover (HT) assumes that the fractional loss of tracer mass represents the fractional loss of stream flow to the subsurface and does not enter the stream channel again during the duration of the experiment (Payn et al., 2009; Covino et al., 2011). Gross losses (Q_{Loss}) were calculated by:

$$Q_{Loss} = Q_{i-1}\frac{M_i - \int_0^t M(t)dt}{M_i} \tag{2}$$

Net discharge changes (ΔQ) and HT were then determined as:

$$\Delta Q = Q_{Gain} + Q_{Loss} \tag{3}$$

$$HT_a = |Q_{Loss}| + Q_{Gain} \tag{4}$$

The absolute differences in Q (ΔQ, eq. 3) between upstream and downstream discharge measurement sites in combination with Q_{Loss} (eq. 2) results in Q_{Gain} as the residual, i.e. the part of ΔQ which is not explained by Q_{Loss} (eq. 2). Finally, HT is normalized to a relative value based on reach length (d) in m:

$$HT = \frac{\frac{HT_a}{Q_{i-1}} 100}{d} \tag{5}$$

2.2.2 The Hysteresis Index

The hysteresis index (h-index) quantifies differences in water levels between rising and falling limbs of a hysteresis loop and is calculated in four steps (Zuecco et al., 2016). The extraction of stream water level data was done manually. Computation is done by utilizing the python script established by Jehn (2019, https://github.com/zutn/Hysteresis-Index-Zuecco). The script contains all computational steps as follows:

Normalization:

$$u(t) = \frac{x(t) - x_{min}}{x_{max} - x_{min}} \tag{6}$$

$$v(t) = \frac{y(t) - y_{min}}{y_{max} - y_{min}} \tag{7}$$

Integral computation for rising ($A_{r[i,j]}$) and falling ($A_{f[i,j]}$) limbs, with A as area of the normalized Integral:

$$A_{r[i,j]} = \int_i^j v_r\,(u)du \tag{8}$$

$$A_{f[i,j]} = \int_i^j v_f\,(u)du \tag{9}$$

Difference computation:

$$\Delta A_{[i,j]} = A_{r[i,j]} - A_{f[i,j]} \tag{10}$$

Summation of differences to obtain the h-index:

$$h = \sum_{k=1}^{n} \Delta A_{[i,j]} \tag{12}$$

The h-Index value is quantified by the sum of the area within the normalized loop $\Delta A_{[i,j]}$, where n is the number of chosen intervals. With x as the GW-level and y as the SW-level at time t (Figure 2). Positive h values indicate clockwise hysteresis, while negative values indicate anticlockwise hysteretic behavior. A value equal to zero indicates no hysteresis or a symmetrical eight shaped. The extent of the hysteretic loop is given by the absolute value of h; the larger the hysteretic loop, the further h is away from zero (Zuecco et al., 2016; Gelmini et al., 2022).

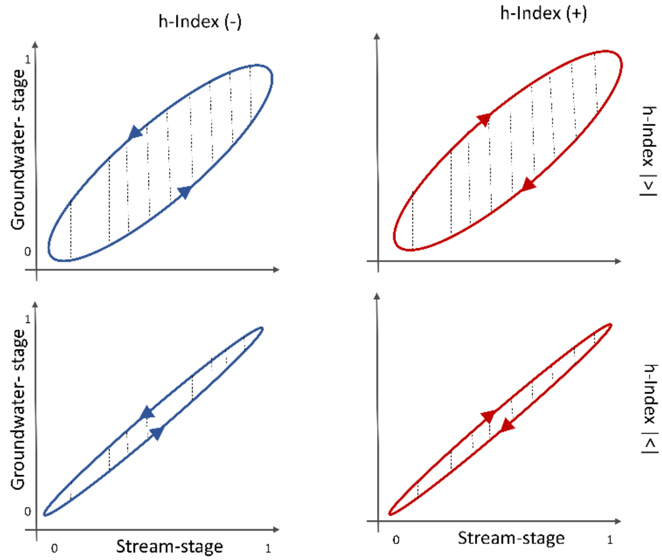

Figure 2: Schematic h-index, with negative index values (blue), counterclockwise rotation. (Red) positive index values, clockwise rotation. Magnitude of area within the hysteresis cycle indicates absolute index value, extended area index value approaches ± 1, contracted area index value near 0. Dotted lines chosen intervals. Based on Lloyd et al, (2016) & Zuecco et al. (2016).

2.2.3 Local Hydraulic Gradient

We assessed the local near stream hydraulic gradients in three different ways. First, we calculated the hydraulic gradient at each time step during the selected hysteresis events. The mean gradient from start to end of the hysteresis event is then associated to the corresponding hysteresis event, resulting in one mean hydraulic gradient per well during each hysteresis event $i_{GW_{(1,2)}}$[-] with, h_S [m] as the mean piezometer height in the stream, $h_{GW(1,2)}$ [m] as the mean piezometer height at the wells GW1 and GW2 and the distance between the stream and the respective well as $d_{(1,2)}$[m].

$$i_{GW_{(1,2)}} = \frac{1}{n} \sum_{k=1}^{n} \frac{h_S - h_{GW(1,2)}}{d_{(1,2)}} \tag{12}$$

Second, we calculated the mean hydraulic gradient $i_{GW_{(1,2)}}$ [-] between both groundwater wells during the defined hysteresis events:

$$i_{GW} = \frac{1}{n} \sum_{k=1}^{n} \frac{h_{GW1} - h_{GW2}}{2.2} \tag{13}$$

3 Results

3.1 Hysteresis behaviour

The majority of the events analyzed in summer showed groundwater levels of the near stream well (GW1) below the stream

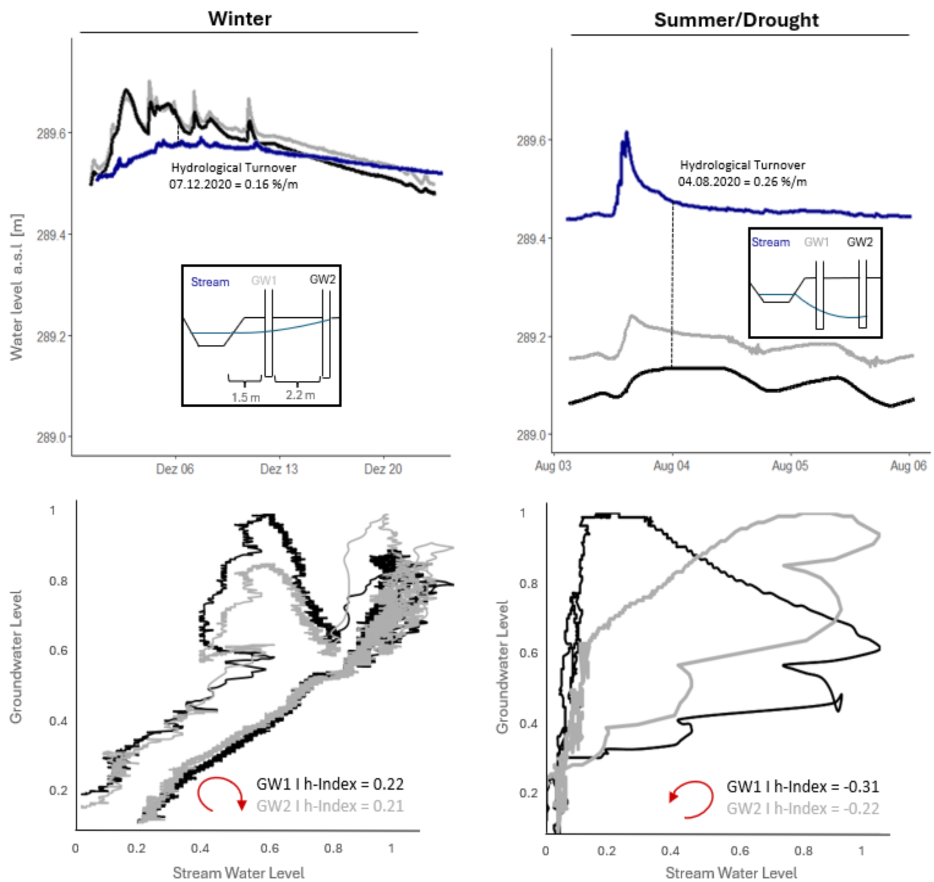

Figure 3: Upper panels: Exemplary events of recorded water-table hysteresis between stream and wells. Left: Characteristic Winter water levels (blue: stream, black: GW1, grey: GW2). Sketch of the experimental setup. Time of HT measurement marked by dashed line. Lower panels: Normalized water levels plotted against each other as hysteretic loops. *h*-Index of the presented hysteretic loops of GW1 (black) and GW2 (grey). Right: Characteristic Summer water levels (blue: stream, black: GW1, grey: GW2). HT measurement marked by dashed line. Normalized water level plotted against each other as hysteric loop. h-indices of the presented hysteretic loops of GW1 (black) and GW2 (grey).

water level (Figure 3). However, in winter groundwater is often observed to be higher than the stream, especially at events during high soil moisture conditions. Analyzing the hysteresis between the stream and the respective groundwater well, we observed differences between hysteretic behavior during all seasons. During summer events the hydraulic head becomes negative, but also the hydraulic head difference between the two observed wells (Figure 3). Precipitation events correspond with the on-site logged hydrograph dynamics as well as the soil moisture data (Figure 4 c).

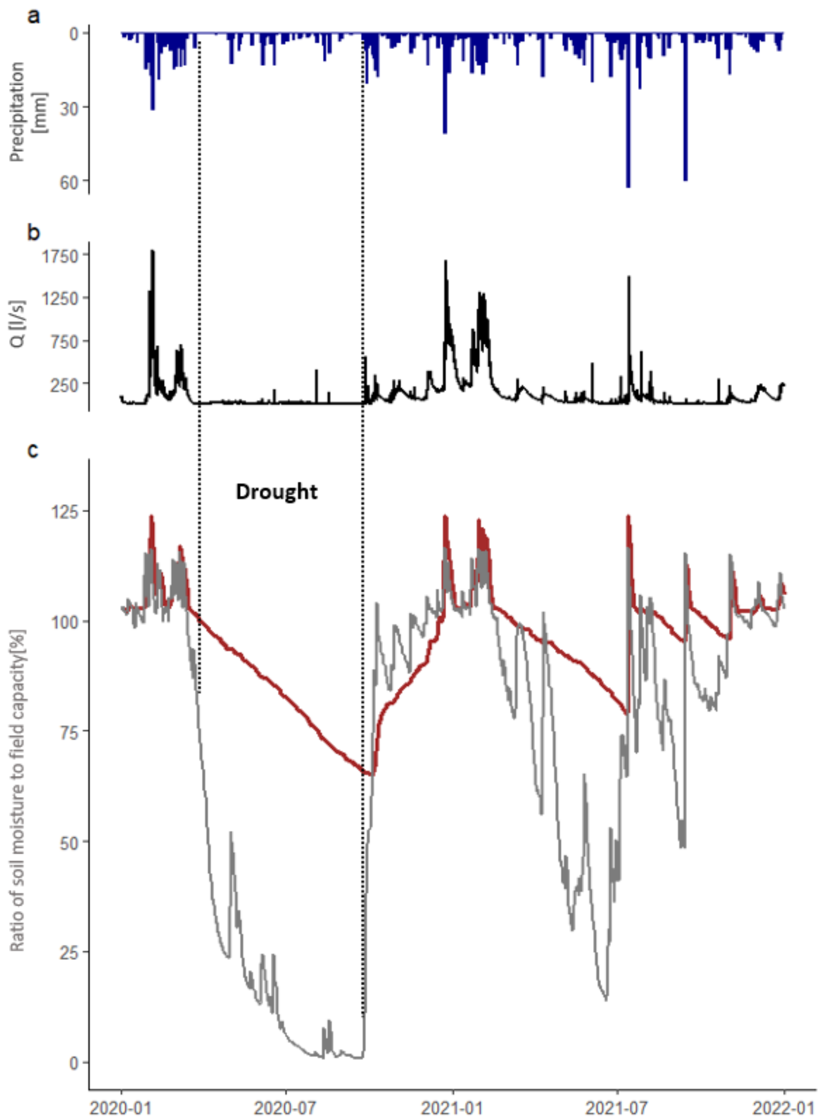

Figure 4: (a) Catchment precipitation (mm) derived from a near weather station. (b) On- site stream flow (l/s). (c) Soil moisture as the ratio to field capacity (-) from a near weather station, two depths: 0-30 cm (grey) and 30-60 cm (brown). Data presented over the observation period, with black dotted lines marking the identified periods of drought;Q below 95% of mean Q (mQ).

Higher catchment soil moisture contents corresponded to higher stream flow and hydrograph reaction velocity to rain events. During drought conditions at stream flow below 5% of mean discharge, we observed the highest HT [%/m] values (Figure 4 & 5), while absolute net exchange presents itself as very low (Figure 5).

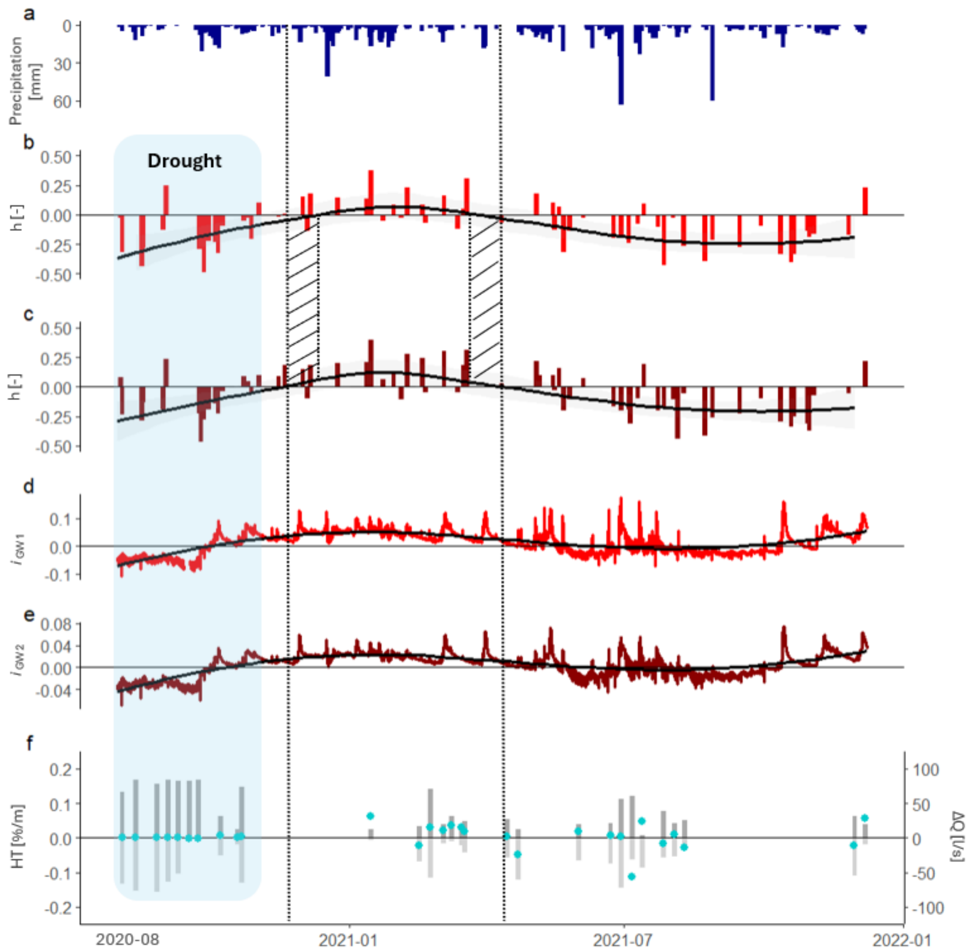

Figure 5: (a) Overview of catchment precipitation (mm) derived from a near weather station. (b) h-Index of hysteresis between stream and GW1 (red), (c) h-Index of hysteresis between stream and GW2 (dark red) with moving average (black line) of index values (n=68) over the observation period. Hydraulic gradient between stream and GW1 (d), GW2 (e), with moving average (black line) of hydraulic gradients (Eq. 13) over the observation period. (f) Hydrological turnover (HT) in %/m point measurements (n= 28) during the observation period. Grey bars indicating net losses and gains, cyan dots net changes. Dotted black lines marking the transitions between summer and winter season. Blue background marks HT measurements during drought conditions (n=9).

We observed extended HT during drought, and distinct seasonality of the h-Index (Figure 5) between winter and summer (including the drought period), with mostly positive index values in summer and negative values in winter. The shift between seasons of the h-Index corresponds with the crossing of its moving average of the zero line (Figure 4 b &c), with h-values during the summer mostly negative (counterclockwise hysteresis) and during the winter positive (clockwise hysteresis) (Figure 3). However, there is a shift in seasonality between the two groundwater wells, with the well closer to the stream (GW1) showing the seasonal shift earlier and transitions later in the year compared to the second well (GW2). The distance between wells is 2.2m, which appears to correspond to one month in delay. Summer rainfall events show a marginal impact on low flows, just initializing sharp spikes in stream flow for a very short period (Figure 3). During winter, frequent rain events sustain higher baseflow (Figure 4 b). However, the Olewigerbach is during both seasons a highly reactive stream with increased discharge amplitudes (Figure 4 b). Seasonality, reflected in precipitation and soil moisture data, aligns with h-index values and hydraulic gradients at the Olewigerbach (Figure 5).

3.2 Hysteresis Index in relation to HT

Comparing the h-indices, both wells at the experimental site show significant differences (Wilcoxon Signed-Rank Test) in h-indices between summer and winter (Figure 6).

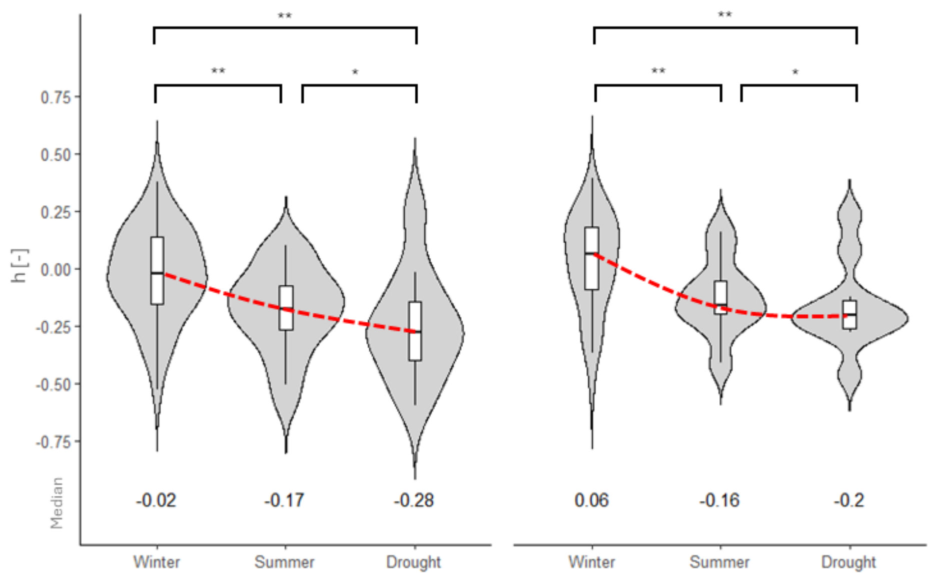

Figure 6: (Left) Violine plots of h-index values (GW1), below median value of the integrated boxplot per season. (Right) Violine plots of h-index values (GW2), below median value of the integrated boxplot per season. Comparison between Winter (n= 37), summer (n=22), and drought (n= 9). Significant difference between groups indicated by * (* p = 0.001, ** p =0.01, * p = 0.05, 95 % confidence interval, Wilcoxon Signed-Rank Test, Holm-Bonferroni). Red dotted line showing decline in median h-index**

The first well tends towards more negative h-index values (counterclockwise) compared to the second well. Seasonally, both wells show significant differences between h-index values. During the summer period, the h-Index values present decreasing values, shifting from clockwise to counterclockwise behavior (Figure 6). Additionally, comparing the h-index values tend further towards negative values during the drought periods. However, the drought dataset is small in observed events (n= 9). h-Index values are significantly elevated during drought compared to winter values. Thus, showing the increased extended duration of the total counterclockwise hysteresis between the stream water level and the groundwater level. Comparing summer HT to drought event HT, the significance level of the Pearson correlation decreases from summer to drought (Figure 6). Comparing the h-index values of both wells to HT, as the part of discharge exchanged per distance (%/m), both wells behave similar. h-Index correlates significantly to HT (Figure 7a & b),

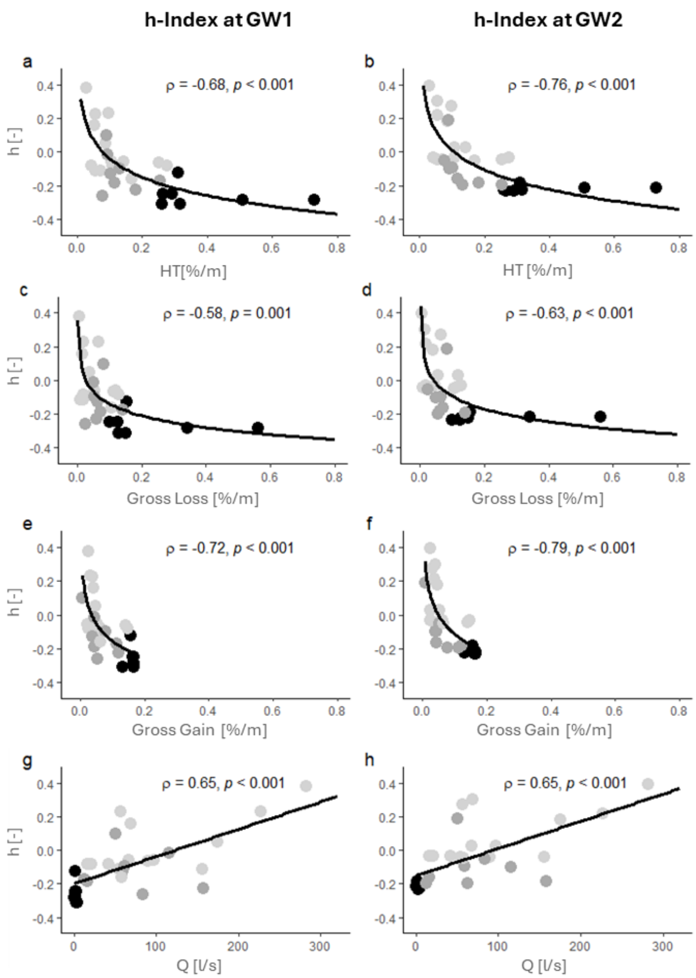

Figure 7: Spearman correlation between h-index value (GW1: left, GW2: right) and HT (a, b), gross loss (c, d), gross gain (e, f) in %/m and discharge (g, h) in l/s. Black data points for drought (n= 7), dark grey for summer (n= 8) and light grey for winter (n= 14).

Also, for the components of HT gross loss (Figure 7c & d) and gross gain (Figure 7e & f). A comparable pattern is evident across all presented correlations: drought measurements cluster at the lowest levels of the h-index range, showing the highest observed HT values (Figure 7). These drought measurements were taken during periods of lowest discharge, whereas winter measurements correspond to periods of highest discharge. Additionally, we observe a positive correlation between discharge and h-index values at both wells (Figure 7g & h).

3.3 Hysteresis Index in relation to Hydraulic Gradients

The mean hydraulic gradient between groundwater wells and the stream during single events, defined as negative toward the stream, shows a significant negative correlation with h-index values (Figure 8a & b; Eq. 12). Steeper negative gradients and more negative h-index values were primarily observed during summer and drought events. In contrast, winter events exhibited both clockwise and counterclockwise hysteresis under less steep gradients.

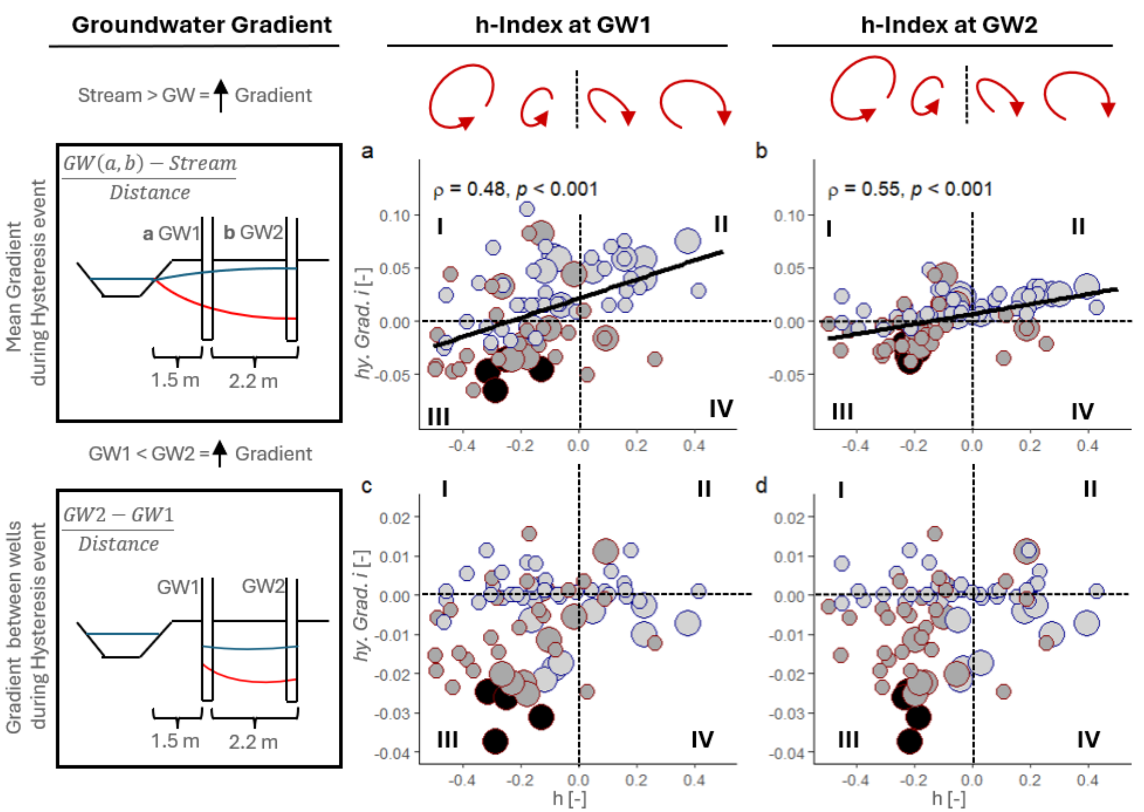

Figure 8: Left: Schematic of hydraulic gradient. Right: Hysteresis direction indicated by red arrows. Mean hydraulic gradient against h-index values at GW1 (a) and GW2 (b) of the hysteresis event (n=68). Hydraulic gradient between GW1 and GW2 against h-index values at GW1 (c) and at GW2 (d). Dot size indicating corresponding HT measurements. Light gray blue couture (Winter), dark grey and red couture (Summer), black (drought). Plots are separated in quadrants: (I) Gaining & counterclockwise; (II) Gaining and clockwise; (III) Loosing & counterclockwise; (IV) Loosing & clockwise hysteresis.

Positive gradients generally indicate gaining conditions, while negative gradients reflect losing conditions. Between the wells (Figure 8c & d; Eq. 13), most summer and drought events displayed negative gradients and counterclockwise hysteresis. Based on hydraulic gradient and h-index we divided the observations into four behavioural clusters (I–IV):

- **Cluster I**: Mostly Winter events and heavy summer rain events; characterized by flat or positive gradients and counterclockwise hysteresis (GW rises before SW).
- **Cluster II**: Winter events; positive gradients with clockwise hysteresis (SW rises before GW).
- **Cluster III**: Predominantly summer and all drought events; negative gradients and counterclockwise hysteresis.
- **Cluster IV**: Smallest group; characterized by negative gradients and clockwise hysteresis; stream-GW pairs include four summer events with negative gradients and clockwise hysteresis. Between wells, five winter and two summer events shared these characteristics.

Gradients between wells were generally smaller and showed higher short-term variability during rain events, compared to stream-GW gradients.Based on these mostly seasonal Clusters we grouped the tracers into a conservative mixing set (geogenic silica, Potassium) and a redox-related set to reflect the hypotheses 1&2 as well as 3, respectively: mixing tracers diagnose HT and its seasonal variability in groundwater-surface water exchange. This separation allows redox tracers (DOC, NO_3^-, Fe, Mn) to specifically indicate the biogeochemical response to the several identifiyed exchange paterns. Redox tracers can track redox dynamics as conceptualized by biogeochemical hydrological coupling (Peiffer et al., 2021) and the classical redox sequence in oxygen-limited environments (Zehnder & Stumm, 1988). We emphasize that event metrics are used as hydrological context, while event classification itself is based on hysteresis behaviour.

3.4 Hysteresis Index and Redox dynamics

Hysteretic behavior and the associatet HT induced mixing through the hyporheic zone and the stream bank, allow for exchange of solutes between GW and SW. Hence, we compared the sampling results by distinguishing seasons (Summer and Winter), Hysteresis direction ($h<0$, $h>0$) and hydraulic conditions based on the gradient data (Loosing or Gaining) (Figure 9).

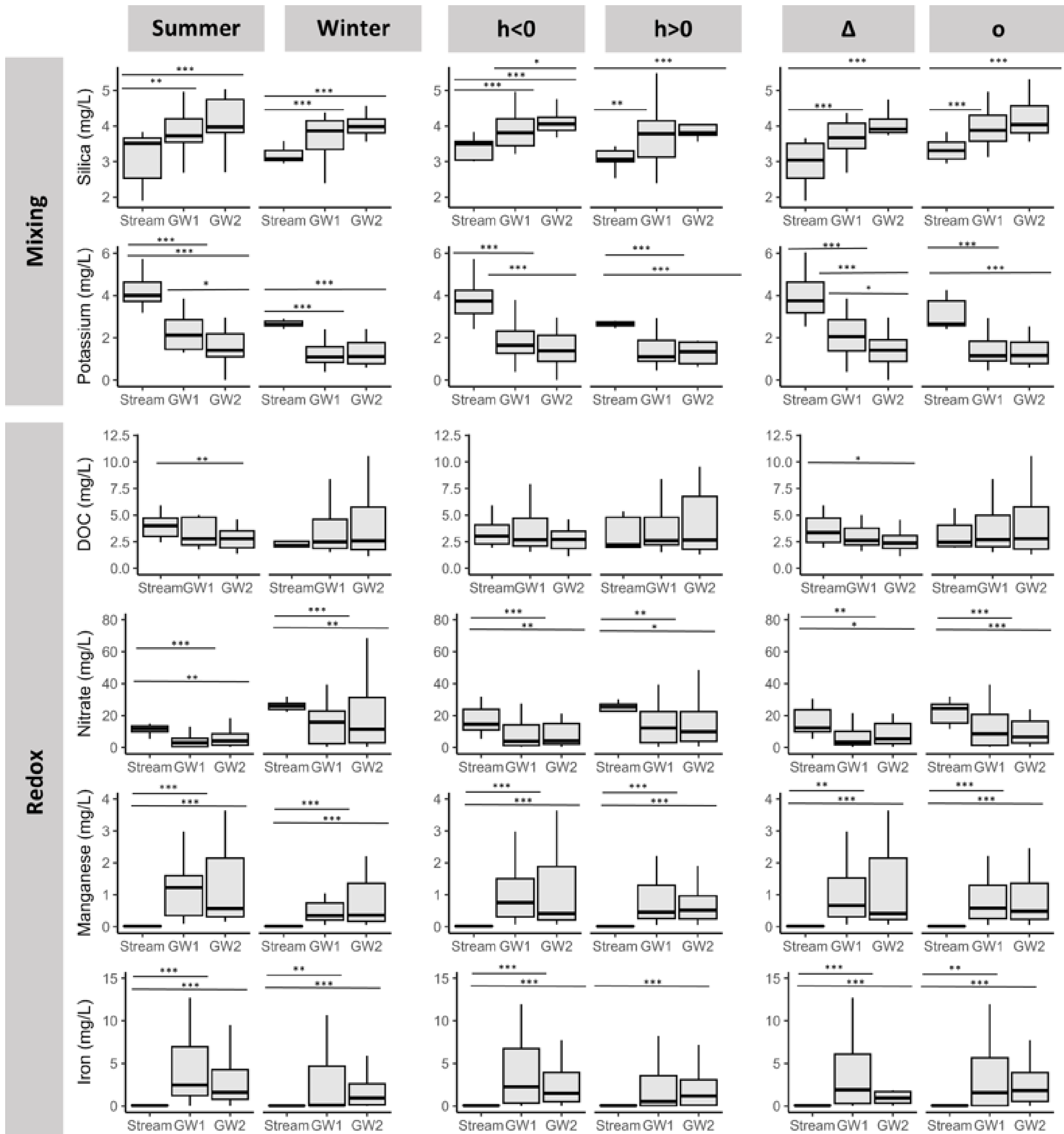

Figure 9: Boxplots of water chemistry parameters separated by (a) season (Summer / Winter), (b) hysteresis direction (h < 0 / h > 0), and (c) hydraulic conditions (Gaining / Losing). (a) Mixing proxies between groundwater and surface water represented by Silica (GW) and Potassium (SW). (b) Redox-sensitive compounds representing the redox chain: DOC, Nitrate, Manganese, and Iron. Significant differences (*p < 0.05, **p < 0.01, ***p < 0.001; Wilcoxon rank-sum test) between the sampling locations Stream, GW1, and GW2 are indicated by stars above the boxplots. Transect between Stream, GW1, and GW2; n = 48

We observed differences for distribution of potassium samples between seasons. The winter events, positive h-Index show consistently the highest values in the stream with similar concentrations in both wells. However, for summer events, negative h-Indices and losing conditions exhibit high potassium values at the stream gradually declining with distance towards the wells. In winter potassium is in a similar range at the wells (Figure 9a). Generally, silica is rising from groundwater to stream in concentration while potassium shows the opposite (Figure 9a). We detected redox-sensitive species (Fe, Mn, NO_3^-) in all samples, with the highest concentrations of iron and manganese consistently observed in near-stream groundwater wells. This suggests heterogeny redox conditions in the riparian groundwater compared to the stream. For DOC concentrations tended to decline from stream to GW during the summer months while the opposite occurred during winter. Nitrate concentrations were generally variable with, on average, higher stream concentrations compared to GW (Figure 9b). Nitrate is constantly present during our observations, regardless of redox potential indicated by the concentrations iron and manganese ions. Manganese and iron are also simultaneously present in comparably high concentrations at the GW wells and show distinct patterns. During summer, manganese and iron concentrations were higher at GW1 compared to GW2, suggesting increased redox activity closer to the stream. These conditions coincided with losing hydraulic gradients and counterclockwise hysteresis, indicating stream-derived organic carbon import may stimulate microbial activity in the near-stream sediments. During summer, losing conditions and with counterclockwise hysteresis manganese and iron concentrations are highest at GW1.

4 Discussion

We utilized the hysteresis index introduced by Zuecco et al. (2016) to analyze changes in the direction and magnitude of hysteresis between stream water levels and groundwater levels at the Olewigerbach catchment. This study relies on two available groundwater wells located in the close vicinity of the stream reach under study. While these wells provide valuable process-based insights into GW–SW exchange and redox dynamics, they cannot capture spatial heterogeneity across the catchment. The geological setting with fissured schists as the near surface bedrock does not provide a contiguous shallow aquifer, and thus no groundwater monitoring network at the catchment-scale. Therefore, larger-scale GW monitoring is absent. We instead utilize the standardized soil moisture model provided by the public weather service for each weather station (DWD) as an alternative proxy for subsurface storage dynamics (Figure 4). Consequently, the conceptual framework we propose (h-index/HT relationships) should be understood as locally constrained and hypothesis-generating, rather than directly representative of larger scales. High-resolution hydraulic gradient data allowed comparison of streamflow events with sufficient resolution to minimize noise. This allowed us to find seasonal variations in hysteretic patterns during the observation period (Figure 6), showing that hysteresis between GW and SW levels are connected to seasonal hydrological states, comparable to those found in the literature (e.g., Zuecco et al., 2016; Lloyd et al., 2016 a; Gelmini et al., 2022).
Although the h-index showed only slight differences in hysteresis between the wells (Figures 3–5), correlation analysis reveals significant spatial and temporal variability in groundwater-stream interactions (Figures 6 & 7). These variations reflect the dynamic nature of the hyporheic zone, which changes seasonally, particularly between winter, summer, and drought conditions (e.g., Wondzell, 2011; Cardenas, 2015; Harvey & Bencala, 1993; Malzone et al., 2016; Wroblicky et al., 1998). As observed

by Gelmini et al. (2022), our study identifies clear seasonality in hysteretic behavior. Specifically, HT varies with seasonal changes in hydraulic gradients and discharge magnitudes (Figures 7 & 8). The h-index serves as an event-based parameter to describe GW-SW interactions by incorporating hydraulic preconditions and event characteristics. Distinct h-index value ranges correspond to increased portions of stream water engaged in turnover processes (Figure 7), aligning with studies emphasizing pressure-head variations and their influence on seasonal groundwater-stream connectivity (Brunner et al., 2009, 2011). The seasonal transition is marked by declining h-index values (including directional reversals) from winter to summer, coinciding with decreasing stream discharge and increasing hydrological turnover. These findings indicate that both the direction and magnitude of hysteresis control the intensity and direction of groundwater–surface-water exchange, as evidenced by the HT measurements. This is consistent with findings from Payn et al. (2009), Covino et al. (2011), and others. Beyond direction, the h-index also reflects temporal dynamics between groundwater and surface water levels during events (Zuecco et al., 2016; Lloyd et al., 2016 b), offering a physical framework for understanding HT processes. Hydraulic gradients between the stream and shallow groundwater serve as preconditions for runoff events, modulating GW-SW interactions (e.g., Zimmer & McGlynn, 2017; Volz et al., 2013) a distinct seasonal pattern emerges, steeper hydraulic gradients during summer events correspond to counterclockwise hysteresis, while gentler gradients in autumn and winter are associated with clockwise hysteresis (Figure 8). This relationship is reflected in our results, where counterclockwise hysteresis (negative h-index) predominantly occurs under steep negative hydraulic gradients, indicating losing conditions, whereas positive or near-zero gradients are commonly associated with clockwise hysteresis and gaining conditions (Figure 8 and corresponding h-index values in Section 3.2). Soil moisture controls the unsaturated hydraulic conductivity, governing occurrence of infiltration and overland flow (Horton, 1933). Thus, controlling threshold behavior and the hydraulic response to rainfall events (e.g. Zehe & Sivapalan, 2009). Based on this hypothesis we identified three system states during the observations, winter, summer and drought conditions. These patterns reflect groundwater storage states and hyporheic zone variability. Hydraulic gradient changes not only influence hysteretic loop direction but also reflect groundwater table dynamics, hyporheic zone extent, and riparian bank storage (e.g., Brunner et al., 2009; Gu et al., 2012; Malzone et al., 2016). Elevated stream stages promote counterclockwise hysteresis and hyporheic zone expansion through increased bankstorage (Gu et al., 2012). Conversely, groundwater discharge initially reduces the hyporheic zone's extent (Cadenas & Wilson, 2007).

Our results demonstrate that dynamic local gradients strongly influence hyporheic exchange fluxes in the form of observed HT magnitude (Figure 8). Thus, the Olewigerbach exhibits distinct seasonal system states that shape the water volume at the surface-groundwater boundary layer and thus shaping exchange in the form of HT. HT significantly correlates with h-Index values, connecting system state driven response with GW-SW exchange. We propose addressing HT as a proportion of total discharge, considering the extent of hyporheic zone involvement relative to streamflow conditions. Under low surface discharge, hyporheic zone expansion potentially increases the ratio of hyporheic area to streamflow, engaging a greater fraction of stream water in HT. This is demonstrated by the observed clustering of hysteresis index and hydraulic gradients reveal distinct hydrological states driven by seasonal conditions and event timing. We show that plotting the events with hydraulic gradient against h-Index value four behavioral clusters can be identified (Figure 8). Cluster I is dominated by winter events with counterclockwise hysteresis and flat or positive gradients, suggests storage influence where groundwater responds ahead of streamflow. This may be indicative of a hyporheic response occurring during early infiltration phases. Cluster II, with winter-dominated events and clockwise hysteresis under gaining conditions, likely indicates surface runoff or upstream input overwhelming the local GW response.

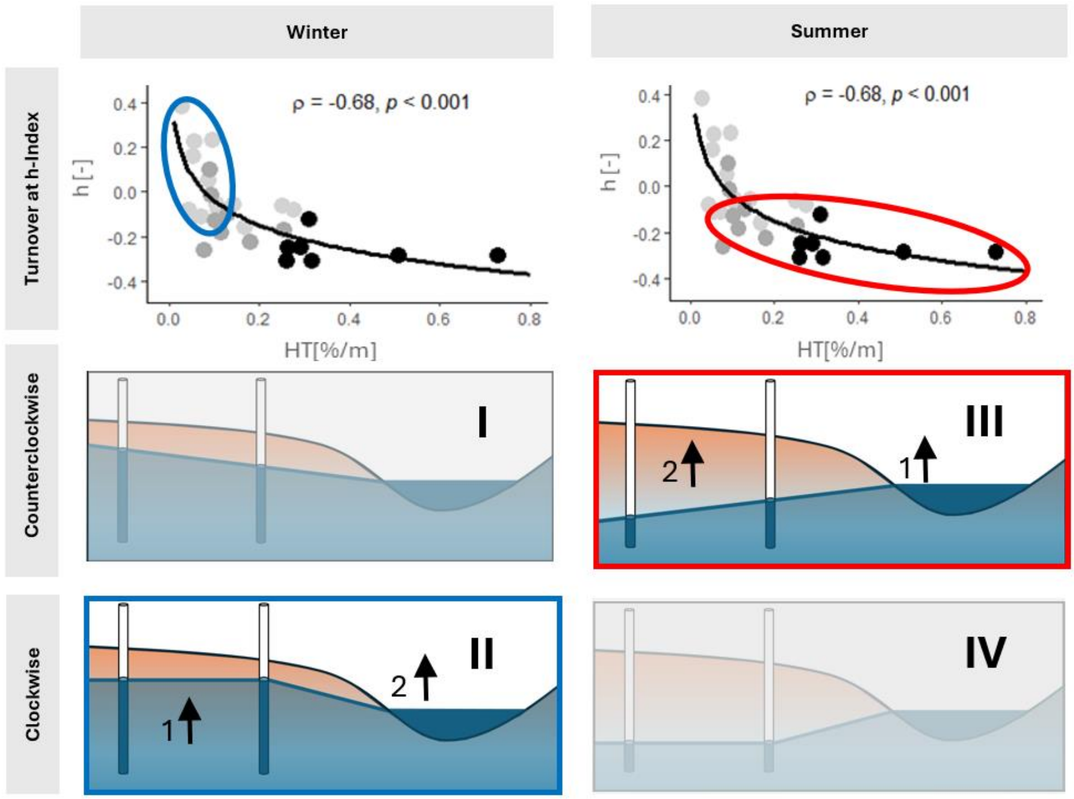

Figure 10: Conceptual comparison of summer and winter conditions at the study site. Top: Seasonal Turnover at h-Index (Summer in red; Winter in Blue). Sketch of the Stream with adjacent groundwater Profile, under clockwise conditions and counterclockwise hysteric conditions. Red frame marking typical summer condition and blue frame marking typical winter

These conditions reduce the influence of subsurface exchange, leading to stream-dominated hysteretic behavior. Cluster III shows the strongest expression of hyporheic connectivity under summer and drought conditions. Steep negative gradients and counterclockwise loops here point to deeper, prolonged infiltration into the Stream bank enabling intense mixing, reflected by the high HT values during those conditions (Figure 7). Cluster IV shows the temporal variability and spatial heterogeneity of riparian processes. Particularly, the flatter gradients between the two wells are more susceptible to transient fluctuations during rainfall events, resulting in mixed hysteresis responses.

Additionally, our results show that gaining and losing conditions are not exclusively associated with one hysteresis direction. Similar observations were reported by Gelmini et al. (2022), who found that hysteresis behavior, captured by the h-index can vary depending on antecedent conditions and event timing, rather than being strictly determined by the direction of exchange. However, this cluster fitted the least number of events during our observed period (Figure 8 & 10). These findings show that combining h-index and hydraulic gradients allows detailed classification of hydrological states at event scale. Also reflected in HT as an independent measure of exchange. Counterclockwise hysteresis and high HT are associated with enhanced riparian bank storage. Vertical expansion of the hyporheic zone at Olewigerbach is likely limited by shallow sediments and small stream size (Malzone et al., 2016). Instead, horizontal bankstorage expansion dominates, forming storage capacities (Figure 10) along the streambank (Gu et al., 2012).

The occurrence of bank storage is associated with counterclockwise hysteresis between stream water and groundwater levels, which occurs primarily during summer (Cluster III), while winter is dominated by clockwise hysteresis patterns (Figure 10). This is further promoted by the losing conditions observed at the site, as similarly described in the Selke catchment (Trauth et al. 2015). Short-time alternating water level gradients during and after stream flow events create oxic-anoxic transition zones in the riparian zone could promote microbial processes (Knorr et al., (2009). Thus, these transition zones created by redox fluctuation within the riparian zone are shaping redox hot spots. This is supported by elevated concentrations of DOC, Fe^{2+}, and Mn^{2+} at GW1 during summer losing conditions, fitting with the concept of the hydrological framework of redox-active compounds in aquatic systems explaining the simultaneous occurrence of ions along the redox ladder Thus, our observed enhanced biogeochemical activity is likely to be driven by redox fluctuations (Figure 9). Such conditions influence chemical turnover, pollutant degradation and solute transport. In redox-sensitive environments, such as the riparian zone microbial reduction processes are understood to occur in a sequence with electron acceptors becoming progressively depleted (Zehnder & Stumm, 1988). This sequence is influenced by factors such as redox potential, pH, electron acceptor availability, and the presence of bioavailable organic matter. While our study lacks direct measurements of dissolved oxygen (DO) and pH, which would have strengthened the interpretation of redox processes, we infer redox conditions based on observed concentrations of DOC, Fe^{2+}, and Mn^{2+}. Although the significance tests indicate that DOC concentrations are comparable across the sampling sites and that Fe^{2+} and Mn^{2+} do not differ significantly between the groundwater wells, we interpret that, during summer and under counterclockwise hysteresis conditions, microbial activity is increased. Thus, during summer and under counterclockwise hysteresis conditions the increased microbial activity and oxygen depletion is based on the co-occurrence of high DOC concentrations, elevated Fe^{2+} and Mn^{2+} in GW1 during losing conditions and counterclockwise hysteresis, likely driven by enhanced inflow of labile organic carbon from the stream into near-stream sediments (Smith & Arah, 1986). This is evidenced by elevated DOC concentrations and redox-sensitive solutes at GW1 (Figure 9). However, our observations revealed the co-occurrence of nitrate, manganese, and iron in groundwater and stream samples. This simultaneous presence of multiple electron acceptors suggests that the redox sequence is not strictly adhered to under field conditions a finding consistent with Alewell et al. (2008) and others. Such deviations from idealized zonation likely result from heterogeneous flow paths, dynamic hydraulic gradients (Peiffer et al., 2021; Frei et al., 2012 and Knorr et al., 2009), and continuous mixing at the GW-SW interface (Gu et al., 2012). Such conditions foster overlapping redox states, enabling parallel rather than sequential redox processes. This highlights the riparian zone as a hydrologically and biogeochemically active layer, supporting diverse redox environments (e.g. Hill & Cardaci, 2004; Carlyle & Hill, 2001). Our findings emphasize the coexistence of multiple redox processes. The resulting shifts between oxic and anoxic conditions are critical for degrading pollutants and supporting biogeochemical activity in the riparian zone. These dynamics underscore the importance of water-stage fluctuations in enhancing chemical exchanges and microbial activity at the GW-SW boundary (Gu et al., 2012).

5 Conclusion

Seasonal variability in GW-SW interactions at the Olewigerbach is driven by changes in discharge, hydraulic gradients, and hyporheic zone dynamics. Our study highlights the h-index as a diagnostic tool for quantifying seasonal shifts in GW-SW interactions, particularly its strong correlation with HT, shedding light on the mechanisms shaping hyporheic zone dynamics.

We characterized the hysteresis between stream water levels and groundwater levels in two riparian wells over two years, calculating the h-index for 68 events and conducting HT estimations for 28 of these events. The h-index revealed clear distinctions between summer and winter conditions, with drought events emerging as statistical outliers. Importantly, we found a strong correlation between hysteretic behavior, quantified through the h-index, and HT. This highlights the role of the h-index in linking hydrological processes with turnover dynamics, particularly during low-flow conditions. Seasonal hydraulic gradients and their influence on bank storage created additional mixing and reaction spaces, increasing the stream water contribution to the hyporheic zone. Elevated HT aligns with hysteresis loop direction and extent, highlighting the hyporheic zone's dynamic spatial reorganization and its influence on solute transport penetrating the riparian zone and creating microenvironments with overlapping redox states.

Our findings suggest that hysteresis behavior can serve as an indicator of changes in hyporheic zone dynamics associated with HT, particularly during summer droughts. This expansion facilitates enhanced mixing processes, influencing stream chemistry. The chemical transects from the stream through the groundwater wells reinforced the critical role of hydraulic gradients in modulating mixing and connectivity within the riparian zone. Thus, leading to frequent shifts between oxic and anoxic conditions, critical for degrading pollutants and supporting biogeochemical activity.

In the context of future climate change, where prolonged droughts and reduced discharge magnitudes are likely to become more frequent, our study suggests that the hyporheic zone will increasingly sustain nutrient cycling and be a prominent component of GW-SW connectivity in gravel bed rivers throughout central Europe. The patterns of elevated HT and large gross exchanges observed during drought conditions indicate that turnover-induced mixing may dominate solute exchange and reaction processes under such scenarios. Our assessment illustrates a robust framework for advancing our understanding of solute transport and GW-SW dynamics at lower order streams, aiding water management under changing climatic conditions.

Author contributions

LB and TS conceptualized the study. Further, LB collected and analyzed field and Lab data. Both LB and TS contributed to the final version of the manuscript.

Competing interests

The authors declare that they have no conflict of interest.

Acknowledgments

The Authors thank Sven Ulrich for his help during initial data acquisition. The author Lars Bäthke is funded by a PhD-stipend of the Studienwerk Villigst e. V., Germany.

References

Alewell, C., Paul, S., Lischeid, G., & Storck, F. R. (2008). Co-regulation of redox processes in freshwater wetlands as a function of organic matter availability? *Science of the Total Environment*, *404* (2-3), 335-342.

Arntzen, E. V., Geist, D. R., & Dresel, P. E. (2006). Effects of fluctuating river flow on groundwater/surface water mixing in the hyporheic zone of a regulated, large cobble bed river, *River Research and Applications, 22*(8), 937 – 946, doi:10.1002/rra.947

Bäthke, L., & Schuetz, T. (2024). Catchment properties shape seasonal variation in groundwater-surface water interaction—Geogenic silica as a proxy for hydrological turnover induced mixing. *Water Resources Research*, 60(6), e2023WR036120.

Boano, F., Harvey, J. W., Marion, A., Packman, A. I., Revelli, R., Ridolfi, L., & Wörman, A. (2014). Hyporheic flow and transport processes: Mechanisms, models, and biogeochemical implications. *Reviews of geophysics*, *52*(4), 603-679.

Brunner, P., Cook, P. G., & Simmons, C. T. (2009). Hydrogeologic controls on disconnection between surface water and groundwater. *Water Resources Research*, *45*(1).

Brunner, P., Cook, P. G., & Simmons, C. T. (2011). Disconnected surface water and groundwater: from theory to practice. *Groundwater*, *49*(4), 460-467.

Burns, D. A., Plummer, L. N., McDonnell, J. J., Busenberg, E., Casile, G. C., Kendall, C., ... & Schlosser, P. (2003). The geochemical evolution of riparian ground water in a forested piedmont catchment. *Groundwater*, *41*(7), 913-925.

Camporese, M., Penna, D., Borga, M., & Paniconi, C. (2014). A field and modeling study of nonlinear storage-discharge dynamics for an Alpine headwater catchment. *Water Resources Research*, *50*(2), 806-822.

Cardenas, M. B., & Wilson, J. L. (2007). Exchange across a sediment–water interface with ambient groundwater discharge. *Journal of Hydrology, 346*(3-4), 69–80, doi:10.1016/j.jhydrol.2007.08.019.

Cardenas, M. B. (2008). The effect of river bend morphology on flow and timescales of surface water–groundwater exchange across pointbars. *Journal of Hydrology*, *362*(1-2), 134-141, doi: 10.1016/j.jhydrol.2008.08.018

Cardenas, M. B. (2015). Hyporheic zone hydrologic science: A historical account of its emergence and a prospectus, *Water Resources Research, 51 (5)*, 3601–3616, doi:10.1002/2015WR017028.

Carlyle, G. C., & Hill, A. R. (2001). Groundwater phosphate dynamics in a river riparian zone: effects of hydrologic flowpaths, lithology and redox chemistry. *Journal of Hydrology*, *247*(3-4), 151-168.

Cooper Jr, H. H., & Rorabaugh, M. I. (1963). Changes in ground-water movement and bank storage caused by flood waves in surface streams. *US Geological Survey Professional Paper*, B192-B195.

Covino, T., McGlynn, B., & Mallard, J. (2011). Stream-groundwater exchange and hydrologic turnover at the network scale. *Water Resources Research*, *47*(12), doi:10.1029/2011WR010942.

Day, T. J. (1976). On the precision of salt dilution gauging. *Journal of Hydrology*, *31*(3), 293–306. doi:10.1016/0022-1694(76)90130-X.

Gelmini, Y., Zuecco, G., Zaramella, M., Penna, D., & Borga, M. (2022). Hysteresis in streamflow-water table relation provides a new classification system of rainfall-runoff events. *Hydrological Processes, 36*(9), e14685, doi:10.1002/hyp.14685.

Gu, C., Anderson, W., & Maggi, F. (2012). Riparian biogeochemical hot moments induced by stream fluctuations, *Water Resources Research, 48,* W09546, doi:10.1029/2011WR011720.

Harvey, J. W., & Bencala, K. E. (1993). The effect of streambed topography on surface-subsurface water exchange in mountain catchments, *Water Resources Research, 29*(1), 89–98, doi:10.1029/92WR01960.

Hill, A. R., & Cardaci, M. (2004). Denitrification and organic carbon availability in riparian wetland soils and subsurface sediments. *Soil Science Society of America Journal*, *68*(1), 320-325.

Horton, R. E. (1933). The role of infiltration in the hydrologic cycle. *Eos, Transactions American Geophysical Union*, *14*(1), 446-460.

Jähkel, A., Graeber, D., Fleckenstein, J. H., & Schmidt, C. (2022). Hydrologic turnover matters - Gross gains and losses of six first-order streams across contrasting landscapes and flow regimes. *Water Resources Research*, *58*, e2022WR032129. doi:10.1029/2022WR032129.

Jehn, F. U. (2019). Pyton code for the hysteresis index of Zuecco et al. (2016). Repository: https://github.com/zutn/Hysteresis-Index-Zuecco. doi.10.5281/zenodo.3441882.

Jimenez-Fernandez, O., Schwientek, M., Osenbrück, K., Glaser, C., Schmidt, C., & Fleckenstein, J. H. (2022). Groundwater-surface water exchange as key control for instream and groundwater nitrate concentrations along a first-order agricultural stream. *Hydrological Processes*, *36(2), e14507*. doi:10.1002/hyp.14507.

Knorr, K. H., Lischeid, G. & Blodau, C. Dynamics of redox processes in a minerotrophic fen exposed to a water table manipulation. *Geoderma* 153, 379–392 (2009).

Krein, A., & Schorer, M. (2000). Road runoff pollution by polycyclic aromatic hydrocarbons and its contribution to river sediments. *Water Research*, 34(16), 4110-4115.

Lloyd, C. E., Freer, J. E., Johnes, P. J., & Collins, A. L. (2016a). Using hysteresis analysis of high-resolution water quality monitoring data, including uncertainty, to infer controls on nutrient and sediment transfer in catchments. *Science of the total environment*, *543*, 388-404.

Lloyd, C. E., Freer, J. E., Johnes, P. J., & Collins, A. L. (2016b). Testing an improved index for analysing storm discharge–concentration hysteresis. *Hydrology and Earth System Sciences*, *20*(2), 625-632.

Mallard, J., McGlynn, B. & Covino, T. (2014), Lateral inflows, stream-groundwater exchange, and network geometry influence stream water composition, *Water Resources Research, 50*, 4603–4623, doi:10.1002/ 2013WR014944.

Malzone, J. M., Anseeuw, S. K., Lowry, C. S., & Allen-King, R. (2016). Temporal hyporheic zone response to water table fluctuations. *Groundwater*, *54*(2), 274-285.

McCallum, J. L., Cook, P. G., Brunner, P., & Berhane, D. (2010), Solute dynamics during bank storage flows and implications for chemical base flow separation, *Water Resources Research, 46,* W07541, doi:10.1029/2009WR008539.

McGuire, K. J., & McDonnell, J. J. (2010). Hydrological connectivity of hillslopes and streams: Characteristic time scales and nonlinearities. *Water Resources Research*, *46*(10).

Outram, F. N., Lloyd, C. E. M., Jonczyk, J., Benskin, C. M. H., Grant, F., Perks, M. T., & Lovett, A. L. (2014). High-frequency monitoring of nitrogen and phosphorus response in three rural catchments to the end of the 2011–2012 drought in England. *Hydrology and earth system sciences*, *18*(9), 3429-3448.

Patrick Jr, W. H., & DeLaune, R. D. (1977). Chemical and biological redox systems affecting nutrient availability in the coastal wetlands. *Geoscience and Man*, *18*(13), 137.

Pavlin, L., Széles, B., Strauss, P., Blaschke, A. P., & Blöschl, G. (2021). Event and seasonal hydrologic connectivity patterns in an agricultural headwater catchment. *Hydrology and Earth System Sciences*, *25*(4), 2327-2352.

Payn, R. A., Gooseff, M. N., McGlynn, B. L., Bencala, K. E., & Wondzell, S. M. (2009). Channel water balance and exchange with subsurface flow along a mountain headwater stream in Montana, United States. *Water Resources Research*, *45*(11).

Payn, R. A., Gooseff, M. N., McGlynn, B. L., Bencala, K. E., & Wondzell, S. M. (2012). Exploring changes in the spatial distribution of stream baseflow generation during a seasonal recession. *Water Resources Research*, *48*(4).

Peiffer, S., Kappler, A., Haderlein, S. B., Schmidt, C., Byrne, J. M., Kleindienst, S., & Planer-Friedrich, B. (2021). A biogeochemical–hydrological framework for the role of redox-active compounds in aquatic systems. *Nature Geoscience*, *14*(5), 264-272.

Penna, D., Tromp-van Meerveld, H. J., Gobbi, A., Borga, M., & Dalla Fontana, G. (2011). The influence of soil moisture on threshold runoff generation processes in an alpine headwater catchment. *Hydrology and Earth System Sciences*, *15*(3), 689-702.

Phillips, J. D. (2003), Sources of nonlinearity and complexity in geomorphic systems, *Prog. Phys. Geogr.*, 27(1), 1–23, doi:10.1191/0309133303pp340ra.

Smith, K. A., & Arah, J. R. M. (1986). Anaerobic micro-environments in soil and the occurrence of anaerobic bacteria. In *FEMS SYMP. 1986.*

Soulsby C., Youngson A. F., Moir H. J. & Malcolm I. A. (2001). Fine sediment influence on salmonid spawning habitat in a lowland agricultural stream: a preliminary assessment. *Science of The Total Environment*, 265(1-3), 295-307, doi:10.1016/s0048-9697(00)00672-0.

Sparks, D. L., & Huang, P. M. (1985). Physical chemistry of soil potassium. *Potassium in agriculture*, 201-276.

Trauth, N., & Fleckenstein, J. H. (2017). Single discharge events increase reactive efficiency of the hyporheic zone, *Water Resources Research*, *53*, 779–798, doi:10.1002/2016WR019488.

Trauth, N., C. Schmidt, M. Vieweg,S. E. Oswald, and J. H. Fleckenstein (2015), Hydraulic controls of in-stream gravel bar hyporheic exchange and reactions, *Water Resources Research*, 51, 2243– 2263, doi:10.1002/2014WR015857.

Voltz, T., Gooseff, M., Ward, A. S., Singha, K., Fitzgerald, M., & Wagener, T. (2013). Riparian hydraulic gradient and stream-groundwater exchange dynamics in steep headwater valleys. *Journal of Geophysical Research: Earth Surface*, 118(2), 953–969. https://doi.org/10.1002/jgrf.20074.

Ward, A. S., Payn, R. A., Gooseff, M. N., McGlynn, B. L., Bencala, K. E., Kelleher, C. A., Wondzell, S. M. & Wagener, T. (2013). Variations in surface water-ground water interactions along a headwater mountain stream: Comparisons between transient storage and water balance analyses, *Water Resource Research*, *49*, 3359–3374. doi:10.1002/wrcr.2014.

Ward, A. S., Wondzell, S. M., Schmadel, N. M., Herzog, S., Zarnetske, J. P., Baranov, V., Blaen, P. J., Brekenfeld, N., Chu, R., Derelle, R., Drummond, J., Fleckenstein, J. H., Garayburu-Caruso, V., Graham, E., Hannah, D., Harman, C. J., Hixson, J., Knapp, J. L. A., Krause, S., Kurz, M. J., Lewandowski, J., Li, A., Martí, E., Miller, M., Milner, A. M., Neil, K., Orsini, L., Packman, A. I., Plont, S., Renteria, L., Roche, K., Royer, T., Segura, C., Stegen, J., Toyoda, J., Wells, J., & Wisnoski, N. I. (2019). Spatial and temporal variation in river corridor exchange across a 5th-order mountain stream network, *Hydrology and Earth System Sciences*, *23*, 5199–5225, doi:10.5194/hess-23-5199-2019.

Welch, C., Harrington, G. A., & Cook, P. G. (2015). Influence of groundwater hydraulic gradient on bank storage metrics. *Groundwater*, *53*(5), 782-793.

Wondzell, S. M. (2011). The role of the hyporheic zone across stream networks, *Hydrological Process*es, *25*, 3525–3532, doi:10.1002/hyp.8119.

Wroblicky, G. J., Campana, M. E., Valett, H. M., & Dahm, C. N. (1998). Seasonal variation in surface-subsurface water exchange and lateral hyporheic area of two stream-aquifer systems. *Water Resources Research*, *34*(3), 317-328, doi:10.1029/97WR03285.

Xin, P., Wang, S. S., Shen, C., Zhang, Z., Lu, C., & Li, L. (2018). Predictability and quantification of complex groundwater table dynamics driven by irregular surface water fluctuations. *Water Resources Research*, *54*(3), 2436-2451.

Yevjevich, V. M. (1967). *An objective approach to definitions and investigations of continental hydrologic droughts* (Vol. 23, p. 25). Fort Collins, CO, USA: Colorado State University.

Zehe, E., & Sivapalan, M. (2009). Threshold behaviour in hydrological systems as (human) geo-ecosystems: manifestations, controls, implications. *Hydrology and Earth System Sciences*, *13*(7), 1273-1297.

Zehnder, A. J. B., & Stumm, W. (1988). Geochemistry and biogeochemistry of anaerobic habitats. *Biology of anaerobic microorganisms*, 1-38.

Zelenhasić, E., & Salvai, A. (1987). A method of streamflow drought analysis. *Water resources research*, *23*(1), 156-168.

Zimmer, M. A., & McGlynn, B. L. (2017). Bidirectional stream–groundwater flow in response to ephemeral and intermittent streamflow and groundwater seasonality. *Hydrological Processes*, 31(22), 3871–3880. https://doi.org/10.1002/hyp.11301.

Zuecco, G., Penna, D., Borga, M. A. R. C. O., & van Meerveld, H. J. (2016). A versatile index to characterize hysteresis between hydrological variables at the runoff event timescale. *Hydrological Processes*, *30*(9), 1449-1466.

Zuecco, G., Rinderer, M., Penna, D., Borga, M., & Van Meerveld, H. J. (2019). Quantification of subsurface hydrologic connectivity in four headwater catchments using graph theory. *Science of the Total Environment*, *646*, 1265-1280.